AD-A041 815 PHYSICAL SCIENCES INC WOBURN MASS F/G 20/5
LASER SIMULATION OF HYPERVELOCITY IMPACT.(U)
MAY 77 P E NEBOLSINE F44620-74-C-0022
UNCLASSIFIED PSI-TR-92 AFOSR-TR-77-0797 NL

1 OF 1
ADA041 815

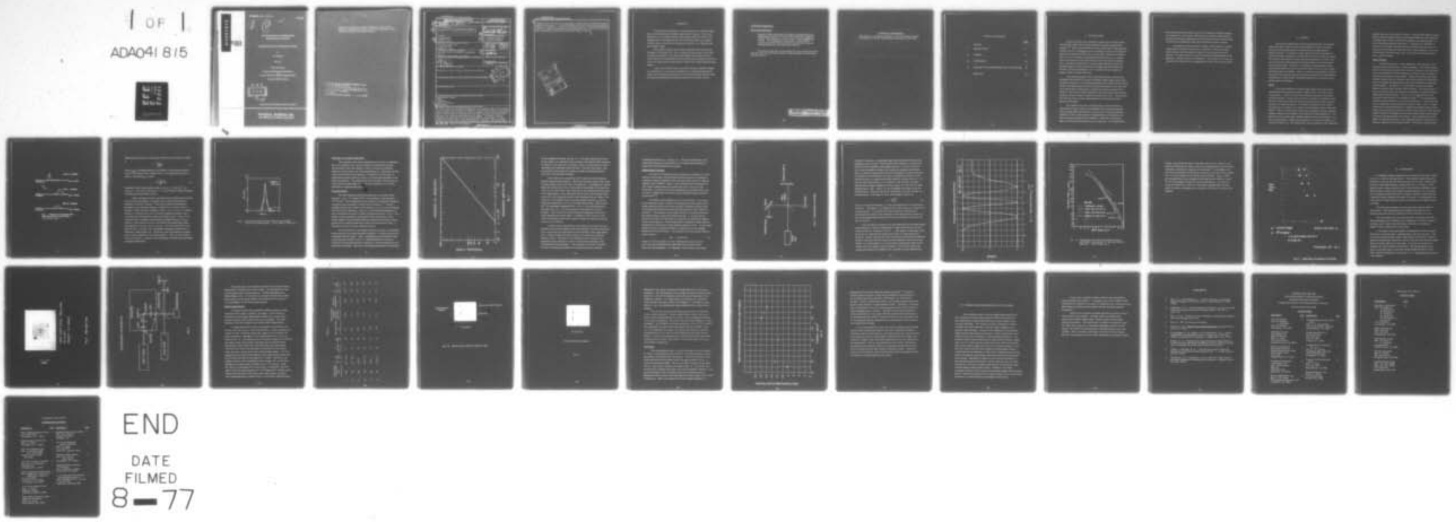

END
DATE
FILMED
8-77

AFOSR-TR-77-0797

PSI TR-92

12

ADVANCED REENTRY AEROMECHANICS

INTERIM SCIENTIFIC REPORT

LASER SIMULATION OF HYPERVELOCITY IMPACT

by

P. E. Nebolsine

May 1977

Jointly Sponsored by

The Space and Missile Systems Organization
and
The Air Force Office of Scientific Research (AFSC)

Contract F44620-74-C-0022

"Qualified requestors may obtain additional copies from the Defense Documentation Center, all others should apply to the National Technical Information Service."

UNCLASSIFIED

SECURITY CLASSIFICATION OF THIS PAGE (When Data Entered)

REPORT DOCUMENTATION PAGE		READ INSTRUCTIONS BEFORE COMPLETING FORM
1. REPORT NUMBER AFOSR-TR- 77-0797	2. GOVT ACCESSION NO.	3. RECIPIENT'S CATALOG NUMBER
4. TITLE (and Subtitle) LASER SIMULATION OF HYPERVELOCITY IMPACT.		5. TYPE OF REPORT & PERIOD COVERED INTERIM Rept.
		6. PERFORMING ORG. REPORT NUMBER PSI-TR-92
7. AUTHOR(s) P. E. NEBOLSINE		8. CONTRACT OR GRANT NUMBER(s) F44620-74-C-0022
9. PERFORMING ORGANIZATION NAME AND ADDRESS PHYSICAL SCIENCES INC 30 COMMERCE WAY WOBURN, MA 01801		10. PROGRAM ELEMENT, PROJECT, TASK AREA & WORK UNIT NUMBERS 2307A2 61102F
11. CONTROLLING OFFICE NAME AND ADDRESS AIR FORCE OFFICE OF SCIENTIFIC RESEARCH/NA BLDG 410 BOLLING AIR FORCE BASE, D C 20332		12. REPORT DATE May 1977
		13. NUMBER OF PAGES 33
14. MONITORING AGENCY NAME & ADDRESS(if different from Controlling Office) 36p.		15. SECURITY CLASS. (of this report) UNCLASSIFIED
		15a. DECLASSIFICATION/DOWNGRADING SCHEDULE

16. DISTRIBUTION STATEMENT (of this Report)

Approved for public release; distribution unlimited.

17. DISTRIBUTION STATEMENT (of the abstract entered in Block 20, if different from Report)

18. SUPPLEMENTARY NOTES

19. KEY WORDS (Continue on reverse side if necessary and identify by block number)

HYPERVELOCITY IMPACE
LASER
SIMULATION
MATERIALS TESTING
SHOCK WAVES

20. ABSTRACT (Continue on reverse side if necessary and identify by block number)

A pulsed laser technique was developed which can simulate single and accurately positioned multiple hypervelocity impacts. Thus, good statistics on many widely spaced single particle impacts and also overlapping craters simulating erosion can be obtained much more quickly and with lower cost than with conventional methods, e.g. light gas guns and ballistic ranges. The present program measured the induced shock duration and strength at the backface of a laser irradiated sample using a laser interferometric technique. The relationship between laser pulse time and shock duration was determined and measured shock

UNCLASSIFIED

SECURITY CLASSIFICATION OF THIS PAGE (When Data Entered) parameters were then used in an approximate scaling model to deduce the surface pressure-time history. A flow and pressure field was formed using the impulsive loading of a material by a laser pulse matching that of a particle hypervelocity impact and indeed the experimental work demonstrated that craters could be made that quantitatively duplicated hypervelocity impact craters.

ABSTRACT

A pulsed laser technique has developed which can simulate single and accurately positioned multiple hypervelocity impacts. Thus, good statistics on many widely spaced single particle impacts and also overlapping craters simulating erosion can be obtained much more quickly and with lower cost than with conventional methods, e. g. light gas guns and ballistic ranges.

The present program measured the induced shock duration and strength at the backface of a laser irradiated sample using a laser interferometric technique. The relationship between laser pulse time and shock duration was determined and measured shock parameters were then used in an approximate scaling model to deduce the surface pressure-time history.

A flow and pressure field was formed using the impulsive loading of a material by a laser pulse matching that of a particle hypervelocity impact and indeed the experimental work demonstrated that craters could be made that quantitatively duplicated hypervelocity impact craters.

ACKNOWLEDGEMENTS

Sponsorship Statement

Research jointly sponsored by the Space and Missile Systems Organization and the Air Force Office of Scientific Research (AFSC), United States Air Force, under Contract F44620-74-C-0022. The United States Government is authorized to reproduce and distribute reprints for governmental purposes notwithstanding any copyright notation hereon.

The author would like to acknowledge the many useful discussions with Dr. Kurt Wray and the assistance of Paul Kingston in performing the experiments.

TABLE OF CONTENTS

I. INTRODUCTION

Physical Sciences has developed a pulsed laser technique which can simulate single and accurately positioned multiple hypervelocity impacts.[1,2] Thus, good statistics on many widely spaced single particle impacts and also overlapping craters simulating erosion can be obtained much more quickly and with lower cost than with conventional methods. Also, we are not limited to precipitation size particles (i.e., greater than 100 microns) but can easily simulate cloud size particle impacts (i.e., less than 100 microns). It is well known that these cloud size particle impacts cannot be performed at single particle facilities and therefore the laser technique is more versatile and also capable of a greater range of impact velocities.

The present program measured the induced shock duration and strength at the backface of a laser irradiated sample using a laser interfermetric technique. The relationship between laser pulse time and shock duration was determined and measured shock parameters were then used in an approximate scaling model to deduce the surface pressure-time history. Much more accurate predictions could be made using numerical computer codes, but this is outside the scope of this work. This information will then allow accurate determination of the equivalent impact particle parameters.

The validity of the laser technique being a good simulation of hypervelocity impact relies on the principle of late stage equivalence. This principle states that identical craters can be formed by different impacts if, before strain rate and strength effects are important, the flow and pressure fields become identical. Therefore, the precise details of the early time history are not important. It is expected that

that a flow and pressure field can be formed using the impulsive loading of a material by a laser pulse matching that of a particle hypervelocity impact and indeed the experimental work demonstrated that craters could be made that quantitatively duplicated hypervelocity impact craters.

A discussion of the simulation concept, impact physics, and past experimental results are discussed in Section II, as well as the laser interferometer and the methods to obtain the surface pressure-time history. The experiment is discussed in Section III giving details on the apparatus, results, and data interpretation. The results of our work are summarized in Section IV and suggestions for future work are also given.

II. THEORY

The previous experimental effort demonstrated that a Q switched ruby laser beam created craters in both brittle and ductile materials which had all the appearances of those made by real hypervelocity particle impacts. A theoretical model related the laser parameters to equivalent particle parameters and the data was reduced using this model. The reduced data yielded a nominal quadratic dependence of crater mass loss on equivalent impacting particle velocity which is also observed in particle impact data. Therefore, a simulation of hypervelocity impact was demonstrated but it is well known that identical craters can be made by different particle impacts. Hence, to reduce the uncertainty in particle parameters the present program measured the induced shock parameters establishing an experimental relationship between laser parameters and induced shock parameters.

Model

The laser simulation of hypervelocity impact model has several requirements which were discussed in detail in Ref. 2 and will be summarized here. First, the laser beam diameter matches the equivalent particle diameter. Second, the laser beam irradiance is adjusted so that the laser induced pressure matches the one dimensional impact pressure produced in a specified impact. The model developed by Pirri relates the laser beam irradiance to an induced surface pressure and is discussed below.[3] Third, the laser beam pulse time is adjusted so that the induced impulse matches the momentum of the equivalent impacting particle. The third part of the model makes physical sense because in early times, i.e., tens of nanoseconds, a hypervelocity impact is an inelastic collision. At much later times, i.e. 100 nanoseconds, some or even all of the impacting particle and crater mass may be ejected. Thus the final impulse may be greater than the original particle momentum and this has been observed in experiments with the result that the impulse was approximately 1.7 times the original particle momentum.[4] Momentum is conserved by the rebound of particle material and some ejected target material. In summary, the model is to match the early surface pressure, area, and time history of particle impact with a laser induced surface pressure, area, and time history.

Impact Physics

As discussed above, a close duplication of the pressure, area and time history is needed for a viable simulation. The impact physics will now be discussed to predict the necessary pressure, area and time. The one-dimensional pressure induced by a particle impact is given by the well known Hugoniot relationship.[5] Hypervelocity impact has been modeled using numerical computer codes which predict that the particle grows in diameter by approximately 20% when the particle is half-way into the target.[6] Therefore, it is reasonable having the equivalent particle diameter equal the laser beam diameter. The time history of the surface pressure is not available from published computer codes or experimental measurements. However, shock durations have been measured at the backface of an impacted target.[7,8] The approximate method to predict this time is to conserve momentum. This model will now be compared to measurements discussed in Refs. 7 and 8. Prater performed a detailed examination of hypervelocity impact induced shock waves in several types of aluminum alloys and in particular made measurements of the shock strengths and also pulse shapes using a quartz gauge to measure the time history of the shock. Three waveforms from his paper are reproduced in Fig. 1; the impacting particles were 0.635 cm diameter spheres of 2017 aluminum alloy. We will now compare these

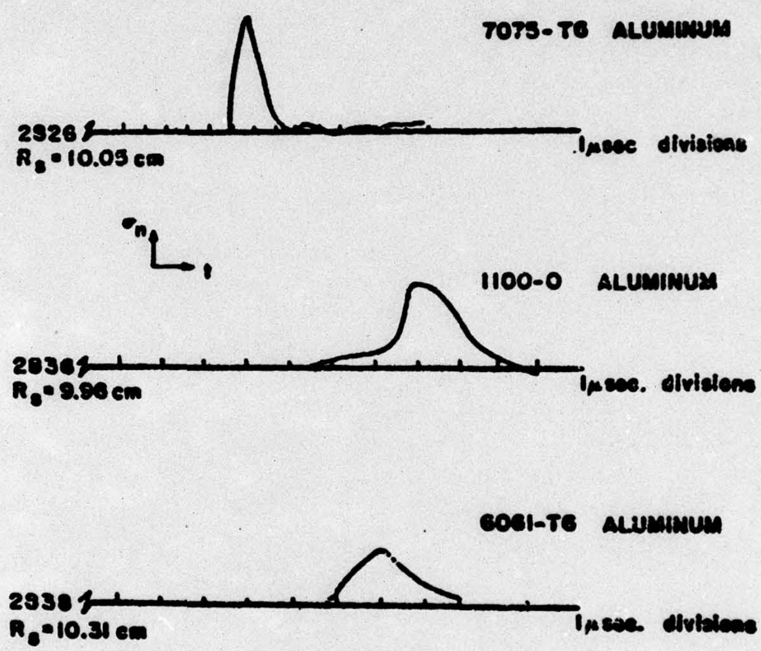

Fig. 1 Waveforms at Large Shock Radii Measured with Quartz Crystal Probes. From Prater Ref. 7

experimental results to our theoretical model for pulse duration τ which is

$$\tau = \frac{m_p v_p}{pA} \qquad (1)$$

where $m_p v_p$ is impacting particle momentum, p is the impact pressure and A is the particle cross sectional area. For spherical particles of radius r and density ρ_p, we have

$$\tau = \frac{4 \pi \rho_p r v_p}{3 p} \qquad (2)$$

Inserting Praten's experimental values, i.e. ($\rho_p = 2.7$ gm/cm^3, v_p = 7 km/s, p = 700 k bar) we find that $\tau = 3.5$ μsec which favorably compares with the pulse times shown in Fig. 1.

Lipkin and Kipp also performed hypervelocity experiments and they measured the perturbation of a sample using a laser interferometric technique to measure velocity.[8] They used a spherical polyethylene projectile and an aluminum target; a sample trace is shown in Fig. 2. Equation 1 yields for their conditions a time τ of 0.31 μsec for an impact velocity of 5 km/sec and 0.125 cm diameter polythylene sphere with p calculated from the Hugoniot relation and Hugoniot data.[5] This is to be compared with a computer code prediction of approximately 0.8 μsec. However, we do note that in Fig. 2 the width of the experimental pulse extrapolated to zero at 2 μsec is 0.6 μsec. We also note that the wave-forms in Fig. 1 and Fig. 2 are all different indicating a dependence on materials, impact speed, etc. Therefore, only very extensive computer codes could be expected to accurately predict τ. Thus, we will continue to use our model for τ because of its simplicity and similarity of predicted and experimental times.

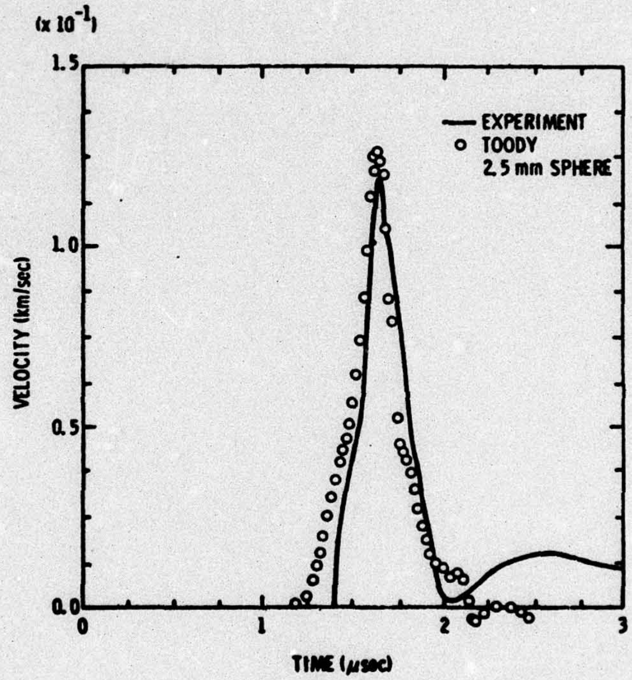

Fig. 2 Comparison of Back-Surface Velocity with TOODY for 2.5-mm-Sphere Impact. From Lipkin & Kipp Ref. 8

Principle of Late Stage Equivalence

The principle of late stage equivalence is the basis for expecting the laser technique to be a good simulation of hypervelocity impact. This principle states that identical craters are formed by different impact if, before strain rate and strength effects are important, the flow and pressure fields become identical. Therefore, the final shape of hypervelocity impact produced craters is not precisely dependent on the impact parameters. It is expected that the flow fields and pressure can be accurately enough duplic..ted b.. the laser technique to be a virtual duplication of hypervelocity impa...

Simulation Model

The laser/material interaction generates a very high surface pressure - e.g., 10^{11} dynes/cm^2 for an irradiance of approximately 10^{11} W/cm^2. Pirri extended the work of Basov to predict the dependence of induced surface pressure on laser beam irradiance.[1,3] Figure 3 graphically shows the results of the model for a 0.7 μm laser wavelength and 100 μm beam diameter. There is a weak functional dependence on laser wavelength and spot size which is discussed in Refs. 1 and 3. The induced surface pressure is proportional to the 7/18th power of the atomic weight of the irradiated material and therefore, induced surface pressures for materials other than carbon can be scaled from Fig. 3. This will be done in our data reduction process.

As discussed above, the Hugoniot equation provides a relationship between particle and target properties yielding a 1-D impact pressure for a specified velocity impact. Thus, combining the laser/material model and the Hugoniot equation, there is a relationship between the laser irradiance and equivalent particle velocity for a known target and equivalent particle material. The mass of the equivalent particle is determined

PRESSURE VS. IRRADIANCE

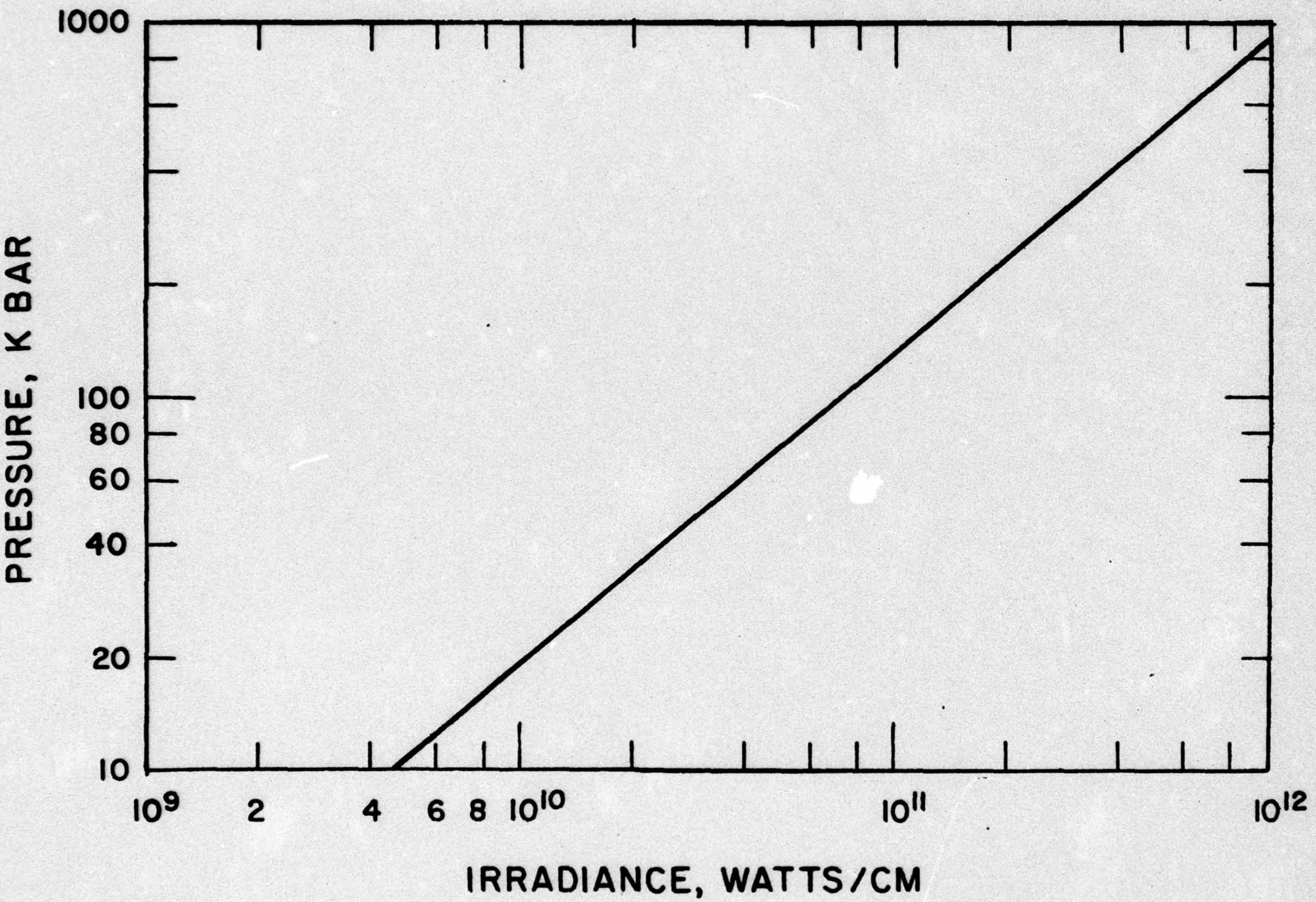

Fig. 3

by the momentum equation (see Eq. (1)). The laser pulse time is used in the model as an estimation of the duration of the induced shock duration. In summary, the laser beam irradiance yields a surface pressure which determines the equivalent impact velocity. The laser pulse time, area, and induced surface pressure combine to yield an equivalent particle mass from the momentum equation.

This model was successfully used to reduce the data during the previous experimental program. Many laser produced craters were made and the average crater mass loss was measured. A convenient non-dimensional parameter used in the erosion physics community is the mass loss ratio, G, the ratio of the crater mass loss to the impacting particle mass. In our experiments, G was determined by the ratio of the average crater mass loss to the equivalent particle mass determined by the model. The values of G were plotted versus equivalent impact velocity, v_p and the exponential dependence of G on v_p was determined using a least squares fit. The exponential dependence was 1.78 ± 0.14 for equivalent glass particles and 1.93 ± 0.16 for equivalent water particles on ATJ-S graphite. This is the same nominal quadratic dependence observed in actual hypervelocity impact tests. In addition to total mass loss, the crater morphology of both laser produced craters and particle produced craters is very similar.

In these earlier experiments, even though the results were very positive, the precise equivalent particle parameters cannot be determined from crater mass loss data because of the principle of late stage equivalence. Indeed, different particle impacts can create extraordinarily similar craters. Therefore, in the present work the induced shock parameters were measured in order to reduce the uncertainty in the equivalent particle parameters. The durations of the shock could then be used to determine the length of the equivalent particle using the momentum equation (i.e., see Eq. (1)). The shock parameters were most easily measured at the backface of a sample whose thickness is larger than the equivalent particle length.

Experimental Technique

A variety of conventional pressure gauges are available for shock pressure and duration measurements but these gauges have inadequate frequency response compared to the laser pulse time which was approximately 40 nsec (FWHM). Hence, a laser interferometric technique was used whose response time was limited only by the rise time of the electronics. We point out that this technology has previously been used in several configurations to measure either sample backface velocity or acceleration[5,8].

The details of the technique will now be discussed. As a result of the simulated impact, a shock wave progresses to the backface of the target material and this shock wave produces a backface velocity which is approximately twice the particle velocity behind the shock within the material[7]. The backface of the sample is used as one of the mirrors in the interferometers shown shcematically in Fig. 4. Because the two optical beams from a He-Ne laser are coherent, an interference pattern occurs on the detector. The interferometer is adjusted to obtain uniform illumination on the detector which optimizes signal to noise. As the sample backface moves, the detector output is modulated due to the changing interference of the two beams. The equation for the normalized detector output voltage is

$$v(t) = 1 - \cos k \, \Delta(t) \quad (3)$$

where k is the wave number of the interferometer laser line and $\Delta(t)$ is the time dependent path length difference between the two legs of the interferometer. For example, if the velocity of the target

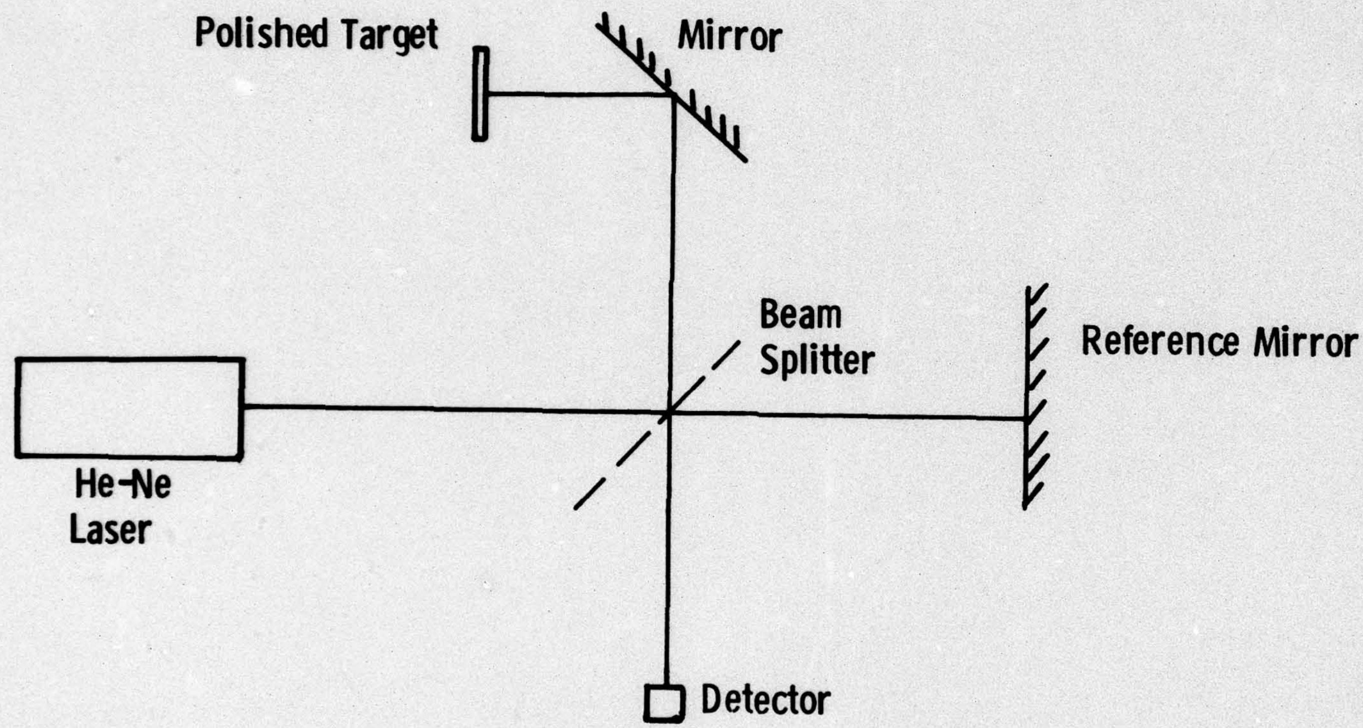

Fig 4. Interferometer Schematic

backface is uniform, a cosinusoidal signal will result with the frequency dependent on the velocity. The duration of the modulation is equal to the duration of the movement of the sample backface. It can be seen from Eq. (3) that nonuniform motions will create non-sinusoidal modulations which can then be interpreted to yield the instantaneous backface velocity. An example was calculated for the case of constant acceleration to peak velocity and then a constant deceleration until the velocity was zero. For this case the displacement, Δ, is quadratic in time and the calculated interferometer fringe amplitude is shown in Fig. 5 for the case of a total displacement of $\frac{9}{2\pi}\lambda$, where λ is the wavelength of the light used in the interferometer. Once the velocity is determined, the shock strength can be determined. If the shock is weak, the strength p is given by

$$p = \frac{\rho C_o U}{2} \tag{4}$$

where ρ is the target density, C_o is the sound speed and U is the backface velocity[9]. The factor C_o is replaced by the shock speed for strong shocks to determine p.[5] In summary, the shock duration is determined by measuring the duration of the modulation of the interferometer signal and the shock strength deduced primarily from the modulation frequency (see Eq. (3) and (4)).

Once the backface pressure has been determined by the experimental measurements, it would be appropriate to relate the backface to a front surface pressure. However, no simple models appear to adequately model the decay of a hypervelocity impact shock wave as it progresses into a material. Prater found that the shock wave decays differently into different alloys of aluminum with the same projectile material, mass and velocity. Figure 6 is a reproduction of one of his figures showing his experimental results and also computer code calculations. We note the rather good comparison between the computer code calculation and the experimental

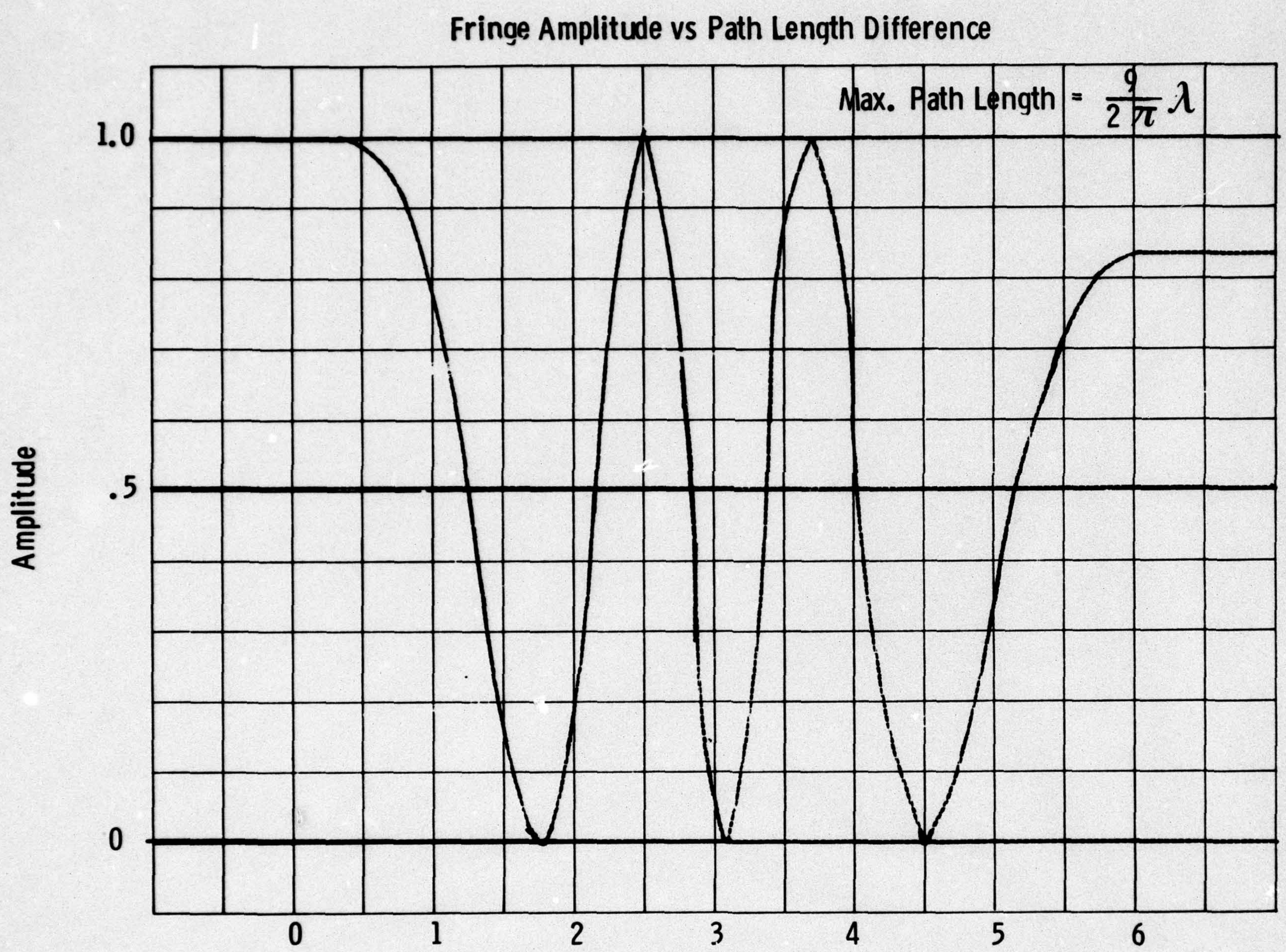

Fig. 5. Path Length Difference $/ \frac{2\pi}{\lambda}$

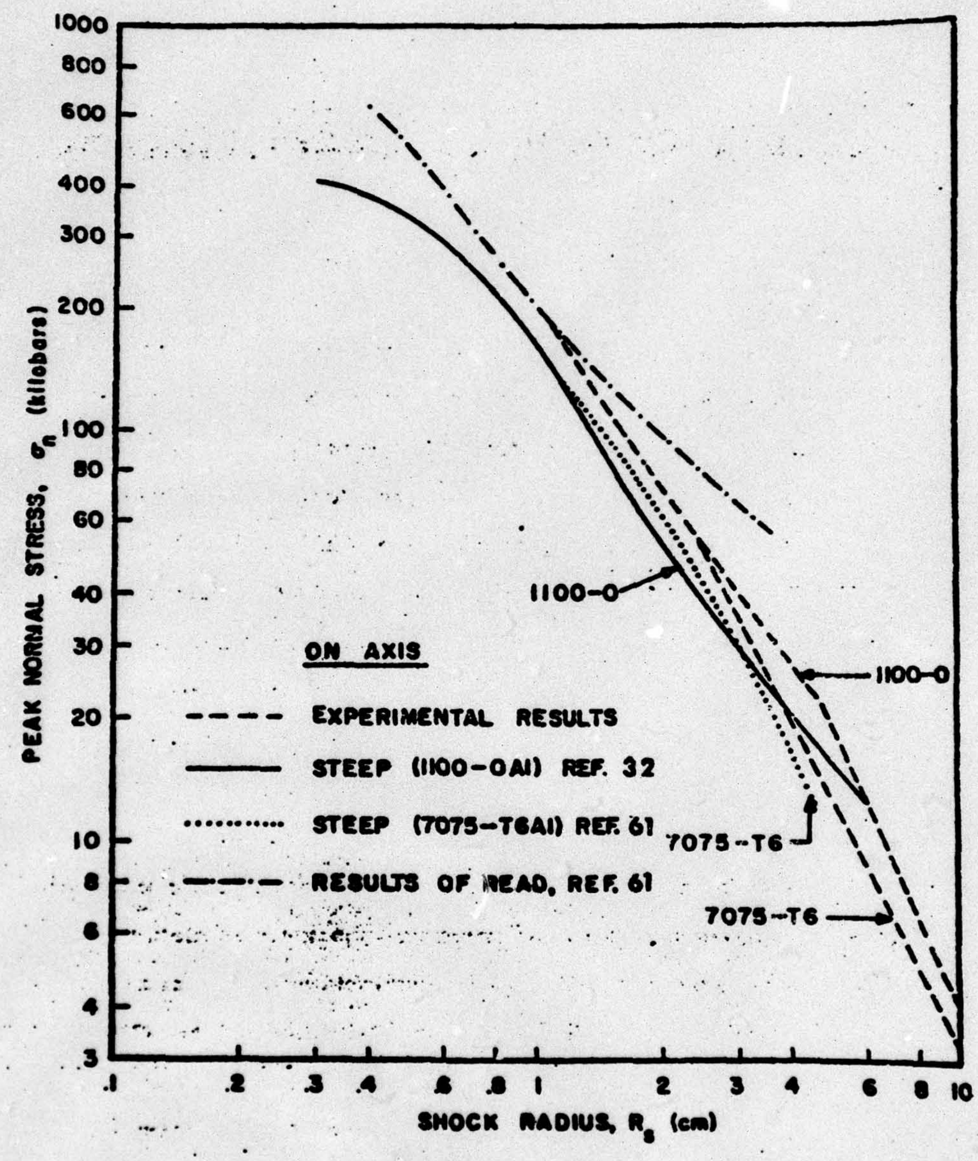

Fig. 6. Comparison of On-Axis Experimental Results with STEEP Code Results -- 1100-0 and 7075-T6 Aluminum. From Prater Ref. 7.

results, particularly the slope of the decay until a shock radius of 4 cm. Lipkin and Kipp provide a good comparison of experimental measurements of backface velocity and computer code prediction.[8] Kreyenhagen et al have made computations of the decay of the shock wave into ATJ-S graphite from 1 cm glass sphere at 12,000 fps impact velocity. Figure 7 shows the calculated peak shock strength versus depth into the material at both 0^{o} and 45^{o} propagation direction from the impact point. We notice the contrast between Fig. 6 and Fig. 7 showing an approximately constant power law decay in aluminum and a non power law decay of the shock into graphite.

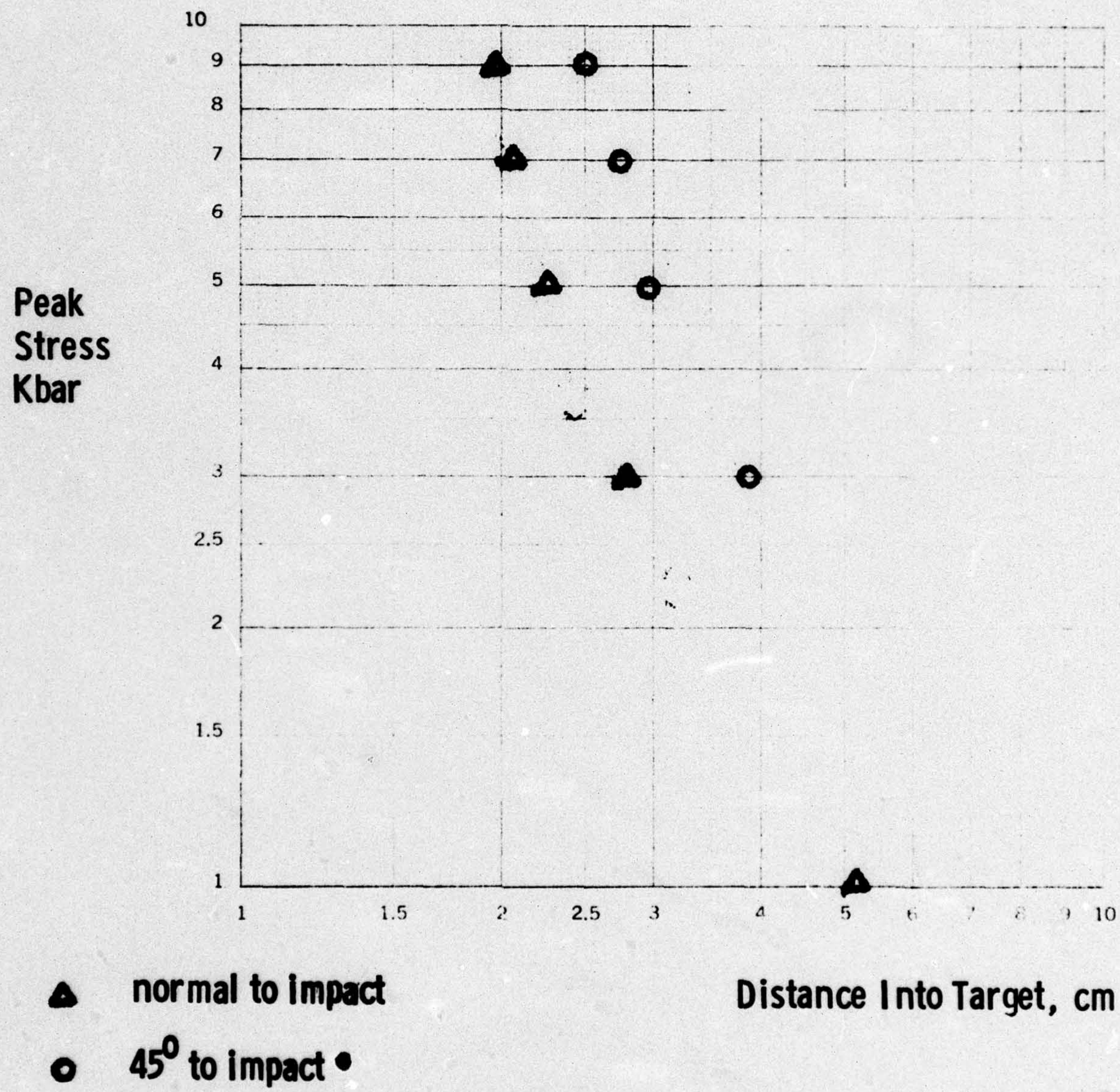

1 cm sphere (glass) into ATJ-S

@ 12,000 fPS

Kreyenhagen, CRT ref. 6

Fig. 7. Peak Stress vs Distance Into Target

III. EXPERIMENT

A Raytheon Company rotating prism Q-switched ruby laser, Model SS-376, was used for the experiments. The maximum output energy was nominally 1 joule and the full width pulse time was 80 nsec. Experiments were done with output energies ranging from 0.2 to 0.4 joules. At the higher energies many transverse modes would oscillate, yielding a rather uniform output irradiance distribution approximately 0.5 cm in diameter. It is a property of high order stable resonator transverse modes that the irradiance declines steeply at the edge of the beam. Near threshold, low order modes oscillated and the decline of irradiance at the edges was not as abrupt.

The laser pulse energy was measured using a Hadron Model 99 Calorimeter. The output voltage was amplified and observed on an oscilloscope and the factory calibration of the calorimeter was used.

The laser pulse time was measured with a fast EG&G SGD-040A silicon photodiode and a Tektronix 475 oscilloscope. The bias voltage on the diode was 90 volts to keep the detector fall-time to a minimum. Figure 8 shows a typical laser pulse shape.

A schematic of the experimental arrangement is shown in Figure 9 showing the ruby laser beam, interferometer, and the vacuum box. The laser beam passed through a glass window placed at Brewster's angle to minimize transmission losses and a lens to focus the beam onto the sample which was held in place by an xyz stage. A vacuum was necessary to prohibit LSD wave formation at the target. The interferometer used a lens in each leg to make a small spot on the sample backface and also obtain uniform illumination on the detector, i.e. constant phase across the 1 mm detector.

Power

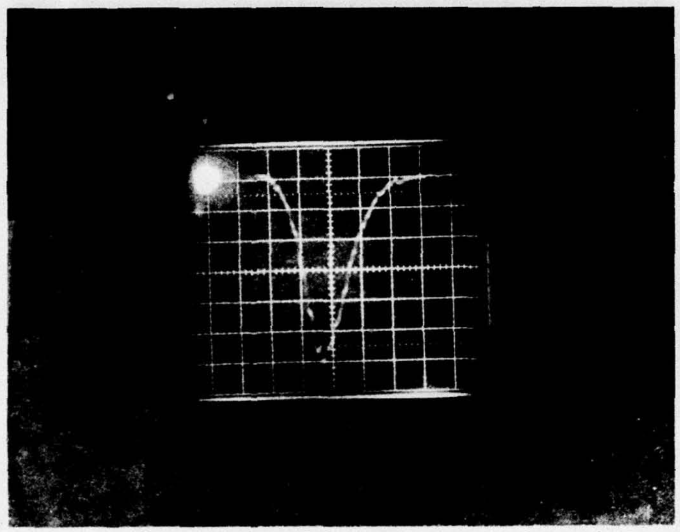

RUBY LASER PULSE, Power vs Time

20 ns/div

ENERGY = 0.5 JOULES

Fig. 8. Ruby Laser Trace

EXPERIMENT SCHEMATIC

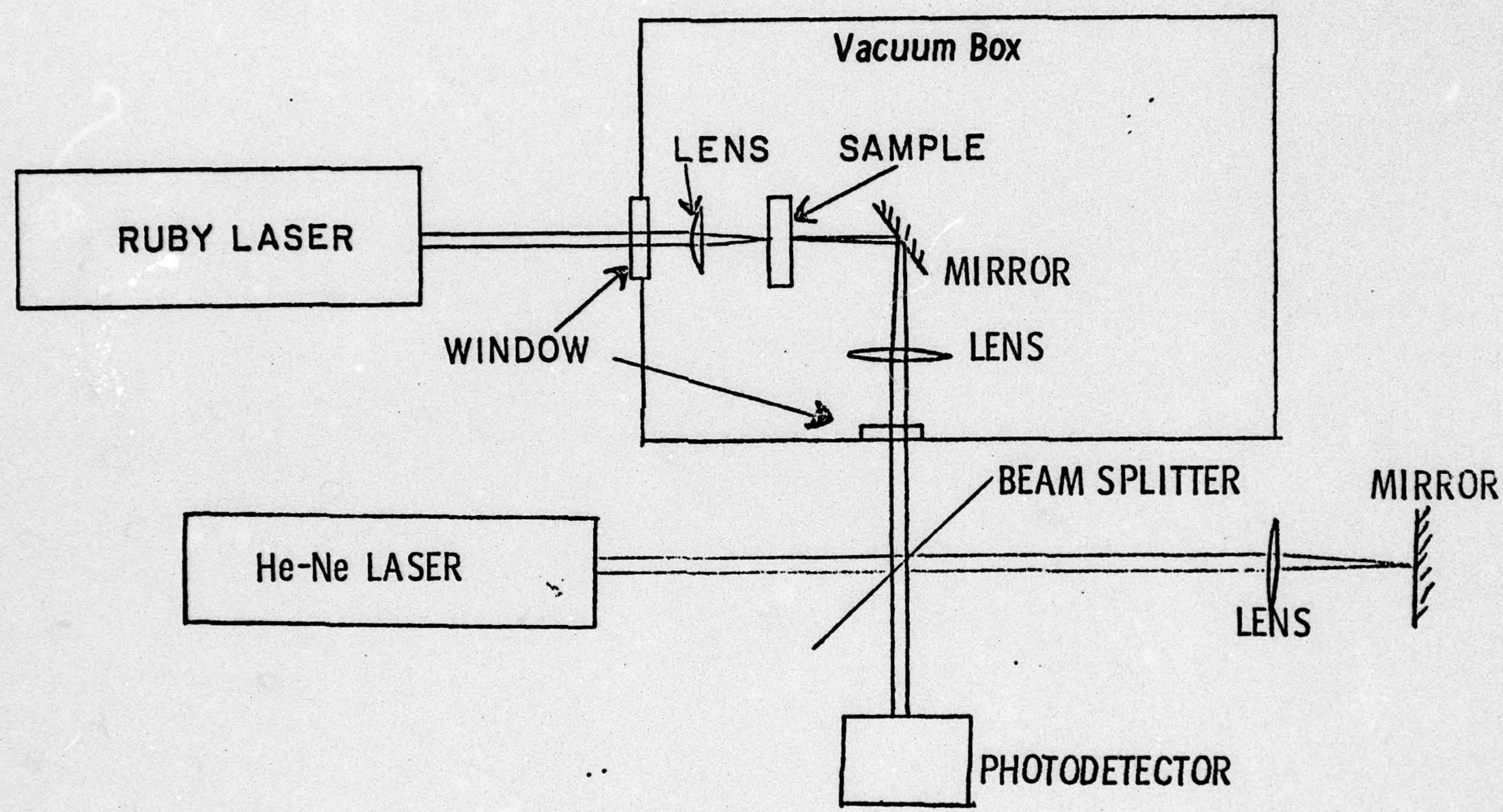

Fig. 9

The small spot on the sample was desired to have the interferometer sense a localized area of the sample. Two photodetectors were used during the course of the program - a silicon photodiode and a photomultipler tube. The best data was obtained with the silicon photodiode using one of the input channels of the Tektronix 475 scope as a 10 x preamplifier for the second input channel.

Experimental Results

A number of tests were conducted on different types of target materials such as glass, graphite, and copper. It was decided to concentrate on the copper experiments because it is a ductile homogeneous material and the back surface can be polished. The other materials would have required more difficult data interpretation.

A copper sample 900 μ thick was polished on the backface and became one of the mirrors in the interferometer. Table I tabulates the results of some of the tests showing the range of shock durations and laser parameters. Examples of two oscilloscope traces, run B, are shown in Fig. 10. The reference beam is blocked in upper trace showing the slight leakage of the intense ruby pulse onto the interferometer photodetector which allows the monitoring of the ruby pulse length. The lower trace shows the ruby pulse, the transit time of the shock wave, 200 nsec, and the shock wave induced fringe change. The overexposed line shows the total amplitude of the interferometer signal and the dot shows the level of over exposure of a point. Therefore, the sample backface can be interpreted to have moved 0.32 μ in 120 nsec yielding an average backface velocity of 2.6×10^2 cm/sec. Using Eq. (4) and a sound speed of 3.6 km/s and $\rho = 8.9$ gm/cm^3, the computed value of the shock pressure is 4×10^8 dynes/cm^2. Similar calculations have been done for the other cases and are given in Table I. Other interferograms are shown in Fig. 11 which show different traces

TABLE I

	Laser Pulse Time, FW ns	E_ℓ J	IP MW	$\overline{I}$ GW/cm^2	P_s Kbar	Shock Duration ns	Ratio of Shock Duration to Laser Pulse Time	Backface Displacement μ	$\overline{U}$ m/s	$\overline{p}$ Kbar
A	100	0.2	2.0	11	38	85	0.85	0.32	3.7	.57
B	90	0.2	2.2	12	44	120	1.3	0.32	2.7	.42
C	110	0.32	3	16	58	130	1.18	0.35	2.5	.39
D	85	0.32	3.8	20	70	155	1.8	.63	4	.62
E	105	0.32	4	21	71	170	1.7	.35	2	.31
F	95	0.42	4.2	22	72	160	1.6	0.55	3.4	.53

Interferometer
Signals

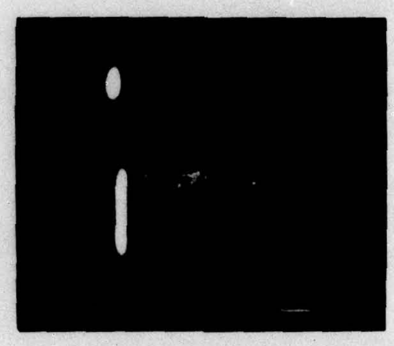

Reference Beam Blocked

Unblocked

100 ns/div

Fig. 10. Interferometer Detector Signal vs Time

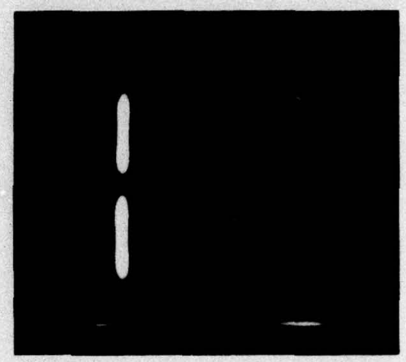

100 nsec/div

Two Interferometer Signals

Fig. 11

dependent on the relative starting path length differences in the interferometer. The interferometer was not rigid so that the mirrors moved slowly (i.e. at audio frequencies) and the precise starting point of the fringe was random - i.e. bright fringe, dark fringe, etc. Because a trace with the ruby beam blocked was straight, i.e. virtually no movement in 1 μsec, the starting path length difference has no effect on the results.

We will now discuss the backface pressure and try to estimate a front surface pressure. Prater's experimental results from Fig. 6 show a decay of approximately 26 to 45 for a shock propagation distance of 7.5 particle diameters, (the ratio of the laser beam diameter to target thickness). The "STEEP" code predicted decays of 30 to 56[7]. If we make the assumption that upper bound of the decay from the "STEEP" code, i.e. 56 is applicable for copper, the front surface pressure loading is predicted to be 17 to 35 kbar for the minimum and maximum cases in Table I. This is to be compared with laser/material interaction model predictions 38 to 72 kbar from Table I. We note that there is a factor of two type of comparison.

Discussion

The measurements shown in the oscilloscope traces and reported in Table I will be plotted to see if there is a correlation between laser parameters and induced shock parameters. The shock duration is most easily determined and has been found to be approximately 0.85 to 1.8 times the laser pulse length. The ratio of shock duration to laser pulse time vs. laser beam irradiance is plotted in Fig. 12. We see the weak correlation of a greater pulse time ratio with increasing irradiance. The pulse stretching can be accounted for by several different physical phenomena such as shock wave stretching and actually longer front surface loading time. Shock wave shape and duration changes dependent on

Ratio of Shock Duration to Laser Pulse Time vs Laser Irradiance

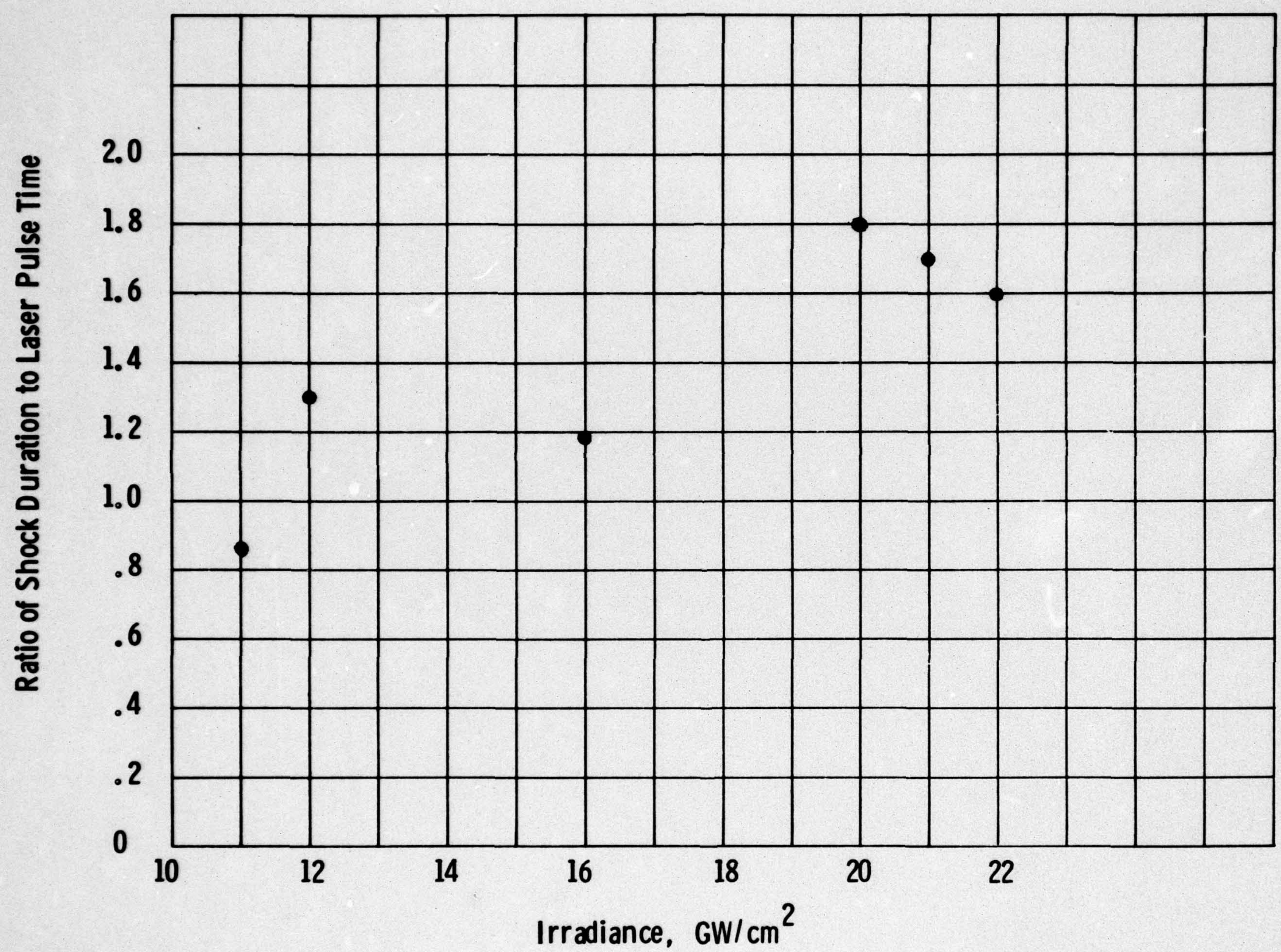

Fig. 12

propagation distance have been theoretically predicted.[5] The laser/material physics predicts a high surface temperature and pressure at the irradiated spot which may take a finite time, e.g. tens of nano-seconds, to decay to much lower values. An acoustic transit time across the laser spot diameter is approximately 20 nsec. Therefore, if the laser beam had abruptly cut off, the surface pressure would at least continue to remain significant for $\geq$ 20 nsec. The time for the surface pressure to reduce substantially is much more difficult to predict but qualitatively it is reasonable that the surface could take a fraction of the laser pulse time to cool enough so that the vaporization rate and therefore vapor pressure was substantially reduced.

An accurate prediction of the front surface loading pressure using backface data is beyond the scope of this work. Obviously a method to evaluate the decay of the shock into the material would be to perform many more experiments with varying target thicknesses and also compare the results to computer code calculations explicitly done for the conditions of the experiments. Even so, the estimates of front surface loading from extrapolations of backsurface data do correspond to predictions of front surface loading from the laser material interaction model. Therefore, there is no doubt that the laser technique does induce strong shocks which are needed to simulate hypervelocity impact.

IV. SUMMARY AND SUGGESTIONS FOR FUTURE WORK

The combined results of the two experimental programs of laser simulation of hypervelocity impact at Physical Sciences Inc. have quantitatively demonstrated that there is good evidence of an accurate simulation. The evidence includes morphology of craters in ductile and brittle materials, mass loss data, spallation, and backface measurements. Because of the ambiguity in the equivalent hypervelocity impact particle parameters, further experiments were needed to reduce the uncertainty in induced shock parameters. The present program demonstrated that the induced shock duration ranged from 0.8 to 1.8 times the laser pulse time which confirms the generation of short high strength shock waves by the laser technique. Also, the front surface pressure was evaluated by extrapolating backface velocity data which yields the correct order of magnitude front surface pressure compared to predictions made with the laser/material interaction model. Analyzing our data for an accurate determination of the equivalent particle parameters of laser produced craters is difficult because of the lack of experimental data for small particle hypervelocity impact produced shock waves. Therefore, the simple momentum model is used to predict hypervelocity impact shock durations and as a result of this program the duration of the pressure pulse should be taken as 1.5 times the laser pulse length in that model.

Future work is needed to further decrease the uncertainty in equivalent impact parameters. A computer code such as TOODY would undoubtedly be required to accurately correlate the front surface pressure-time history to backface measurements and also equivalent particle parameter[8].

Impulse measurements combined with shock duration measurements would be very fruitful. The data could be correlated with hypervelocity impact impulse data to further reduce the equivalent particle parameters. The impulse data is sensitive to particle momentim while crater mass loss is nominally dependent on particle kinetic energy, this allows the determination of equivalent particle mass and velocity. Thus, as further refinements are made in this technology, this low cost technique will have greater application in materials testing.

REFERENCES

1. Rae, W. J. and Hertzberg, A., "On the Possibility of Simulating Meteoroid Impact by the Use of Lasers", NASA Report CR-54029, (1964).

2. Nebolsine, P. E., "Laser Simulation of Erosion", Vol. III, Advanced Reentry Aeromechanics Interim Scientific Report, PSI TR-29, Aug. 1975.

3. Pirri, A. N., "Theory for Laser Simulation of Hypervelocity Impact", Phy. of Fluids 20, 221 (1977).

4. Hunt, A., ETI, private communication.

5. Kinslow, R. ed., High-Velocity Impact Phenomena, Academic Press, New York, (1970).

6. Kreyenhagen, K. N., Wagner, M. H. and Goerke, W. S., "Direct Impact Effects in Hypersonic Erosion", Report No. CRT-5000-1, California Research and Technology, Woodland Hills, CA, (1973).

7. Prater, R. F., "Hypervelocity Impact-Material Strength Effects on Crater Formotion and Shock Propagation in Three Aluminum Alloys", Dec. 1970 AFML TR-70-295 and also AD 718461 at NTIS.

8. Lipkin, J. and Kipp, M. E., "Wave Structure Measurement and Analysis in Hypervelocity Impact Experiments", J. of App. Physics 47, 1979 (1976).

9. Zel'dovich, Ya. B. and Raizer, Yu P., "Physics of Shock Waves and High-Timperature Hydrodynamic Phenomena", Academic Press, New York (1967).

DISTRIBUTION LIST FOR
ADVANCED REENTRY AEROMECHANICS
INTERIM SCIENTIFIC REPORT
"LASER SIMULATION OF HYPERVELOCITY IMPACT"

Contract F44620-74-C-0022

CONTRACTORS

RECIPIENT	CYS
Avco Corporation Attn: W. Rieneke V. DiCristina 201 Lowell Street Wilmington, MA 01887	2
McDonnell Douglas Astronautics Co. Western Division Attn: L. Cohen 5301 Bolsa Avenue Huntington Beach, CA 92647	1
Philco-Ford Western Aeronautics Division Western Development Labs. Attn: Robert Lyons Ford Road Newport Beach, CA 92663	1
Prototype Development Associates, Inc. Attn: John Slaughter Suite 201 1740 Garry Ave. Santa Ana, CA 92705	1
Science Applications, Inc. Attn: C. W. Busch 101 Continental Bldg, Suite 310 El Segundo, CA 90245	1
California Research and Technology Attn: K. N. Kreyenhagen 6269 Variel Avenue, Suite 200 Woodland Hills, CA 91364	1
Martin-Marietta Corp. Orlando Division Attn: Bill Gray P. O. Box 5837 Orlando, FL 32805	1
Lockheed Missile and Space Co., Inc. Attn: T. R. Fortune Continental Bldg. Suite 445 101 Continental Blvd. El Segundo, CA 90245	1
Research and Development Assoc. Attn: A. Field P. O. Box 3580 Santa Monica, CA 90403	1
Physical Sciences, Inc. Attn: Dr. Weiss 30 Commerce Way Woburn, MA 01801	1

Distribution List (Cont'd)

CONTRACTORS

RECIPIENT	CYS
Aerospace Corporation Attn: D. Glenn (1) W. Herbig (4) R. Strickler (1) R. Young (1) M. Masaki (1) W. Grabowsky (1) Library (1) P. O. Box 92957 Los Angeles, CA 90009	10
Sandia Laboratories Attn: Ken Cole P. O. Box 5800 Albuquerque, NM 87116	1
TRW Systems Group Attn: D. Sowers A. Benjamin One Space Park Redondo Beach, CA 90278	2
Acurex Corporation Attn: R. Rindal 485 Clyde Avenue Mountain View, CA 94040	1
General Electric Corp. Attn: Mr. Alan Saydah Bldg. 100, Rm. 3027U P. O. Box 8555 Philadelphia, PA 19101	1

Distribution List (Cont'd)

GOVERNMENT AGENCIES

RECIPIENT	CYS
Naval Ordnance System Comm. Attn: ORD-0333A Washington, D. C. 20360	1
Naval Research Laboratory Attn: W. Atkins Washington, D. C. 20390	1
Air Force Materials Lab. Attn: G. Schmitt (MBE) Maj. Keck (MXS) Wright-Patterson AFB OH 45433	1
Air Force Systems Command Attn: Maj. L. Hillebrand Andrews AFB Washington, D. C. 20331	1
Space and Missile Systems Org. Attn: RSSE/Capt. Jackson (2) RSSE/Maj. Hudack (1) P. O. Box 92960 Worldway Postal Center Los Angeles, CA 90009	3
U. S. Army Missile Comm. Attn: L. Lively Redstone Arsenal Huntsville, Alabama 35809	1
Naval Surface Weapons Center White Oak Laboratory Attn: Dr. Lyons Silver Spring, MD 20910	1
Strategic Systems Proj. Office Attn: Mr. Meserole Crystal City Plaza Arlington, VA	1
U. S. Army Safeguard Systems Command Attn: H. Adams P. O. Box 1500 Huntsville, Alabama 35807	1
Defense Nuclear Agency Attn: Maj. Swartz Capt. Huston Washington, D. C. 20305	2
Space and Missile Systems Organization Attn: MNN/Maj. Jackson Norton AFB, CA 92409	1
U. S. Army Advanced Ballistic Missile Defense Agency Attn: CRDABH-S/W. C. Loomis P. O. Box 1500 Huntsville, Alabama 35807	1